

## Improvement of seismic imaging in a low signal-to-noise area by the use of post-stack stereotomography

I. Panea<sup>1</sup>, E. Landa<sup>2</sup>, G.G. Drijkoningen<sup>3</sup>, R. Baina<sup>2</sup>

<sup>1</sup> University of Bucharest, Faculty of Geology and Geophysics, 6 Traian Vuia Str, RO-020956, Bucharest, Romania and Research School Integrated Solid Earth Sciences (ISES), The Netherlands

<sup>2</sup> OPERA, Rue Jules Ferry, Batiment IFR, 64000 Pau, France

<sup>3</sup> Research School Integrated Solid Earth Sciences (ISES), The Netherlands

---

**Abstract:** *Stereotomography belongs to the slope methods providing a velocity model by traveltime inversion. It can be applied using the traveltimes picked on pre-stack data and post-stack data. In this paper we apply post-stack stereotomography on a land seismic reflection dataset with the purpose to get an accurate 2D velocity. Then, the velocity information is used to perform a pre-stack depth migration using the Kirchhoff method, the same like that one used in the standard processing flow.*

*The post-stack stereotomography results are different than those of the standard processing. The Common-Reflection-Surface (CRS) stack shows some areas where the reflectivity is enhanced, compared to those from the Common-Midpoint (CMP) stack, obtained from standard processing. The 2D velocity model, obtained through the inversion of the picked traveltimes on the CRS stack and verified through the Common-Image-Gathers (CIG) analysis, contains good and reliable velocities that provide a better depth image of the subsurface.*

---

**Key Words:** *Seismic processing, Stereotomography, 2D velocity model*

### Introduction

Stereotomography is a method that determines a macro-velocity model from seismic reflection data (Billette and Lambaré, 1998). It is based on the automatic picking of locally coherent events on pre-stack data (common shot and receiver gathers). Since the automatic picking on pre-stack data characterized by low signal-to-noise ratio does not provide reliable picks, the resulting velocity model can be far away from the true model. Therefore, Lavaud et al. (2004) proposed a modification to stereotomography based on the automatic picking of local coherent

events on post-stack data, namely on a Common-Reflection-Surface (CRS) stack. The optimal wavefront parameters are obtained during the generation of the CRS stack (Jäger, Mann, Höcht and Hubral, 2001); next, the velocity model is determined based on the inversion of the traveltimes picked on the CRS stack. The combination of these two steps is known as “post-stack stereotomography”.

The post-stack stereotomography was applied with good results on synthetic seismic data and marine seismic dataset (Lavaud, Baina and Landa, 2004; Lambaré, Alerini and Podvin, 2004). In addition, the post-

stack traveltimes picking seems to be a robust and reliable procedure commonly used in seismic interpretation (Lavaud et al., 2004). This method belongs to the slope tomography methods proposed during the last decade (Billette and Lambaré, 1998, Chauris, Noble, Lambaré and Podvin, 2002, Duvenek and Hubral, 2002). The stereotomography has been implemented in 2D (Billette, Le Begat, Podvin and Lambaré, 2003) and 3D (Chalard, Podvin, Le Begat, Berthet and David, 2002).

In this paper we focus on a field dataset with a low signal-to-noise ratio. Because of its low signal-to-noise ratio, the velocity analysis performed on the CMP gathers with a standard procedure did not provide a very reliable 2D velocity model. Most of the CMP gathers were avoided during this analysis because of their low desired signal level. Next, the depth migration does not run well because the interval-velocity model derived from the conversion of the stacking velocities is not good enough. Knowing that the signal-to-noise ratio can be improved, also, by stacking of the data it seems that the post-stack stereotomography can be used with good results. In addition, there is a possibility to verify the accuracy of the velocity model by a Common-Image-Gathers (CIG) analysis, during the migration step.

We start the paper with the background on the stereo-tomography method, based on the CRS-stack approach. Then, we introduce the dataset to be used for analysis and comparison between the standard CMP-based approach and the CRS-stereo-tomography approach. These two approaches are then discussed in separate sections. Finally, results and

conclusions are drawn, based on these results.

### Background to post-stack stereotomography

We start the discussion with the Common-Reflection-Surface (CRS) stack since it is intimately related to stereotomography. Post-stack stereotomography uses picked traveltimes on the Common – Reflection - Surface (CRS) stack, so the post-stack domain. The CRS stack gives an accurate zero-offset approximation of the seismic section; in addition, the procedure used to generate the CRS stack is also used to compute the wavefront parameters for each CMP position and time sample (emergence angle of the zero-offset ray and two radii of wavefront curvatures  $R_N$  and  $R_{NIP}$ ). These three parameters are associated with two hypothetical waves namely, the normal wave (N) and the normal-incidence-point wave (NIP). The N and NIP waves, also known as eigenwaves, result from two hypothetical experiments, where a point (diffractor-like) and a reflector are the secondary source in the subsurface. For example, Figure 1 shows a model with three homogeneous layers for these two types of cases. The NIP wave is obtained by placing a point source on a reflector (see Fig. 1, left), so like a point-diffractor, and the N wave is obtained after a simultaneous excitation along a reflector (see Fig. 1, right), so like an exploding reflector. In the vicinity of a point from the acquisition line,  $x_0$ , both wavefronts can be approximated by circles with radii of curvature  $R_{NIP}$  and  $R_N$ , respectively (Jäger et al., 2001).

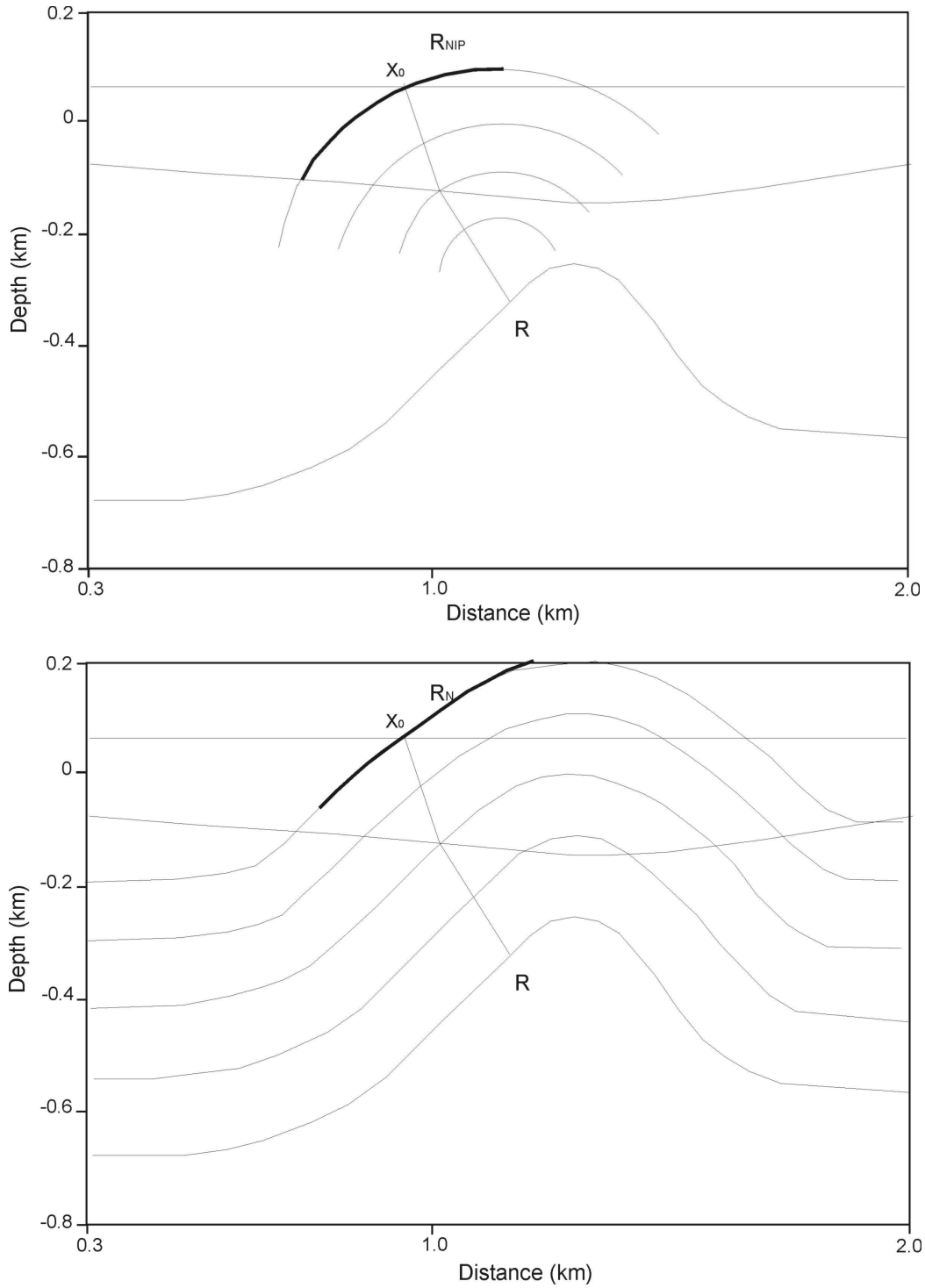


**Fig. 1.** NIP wave for a point source at R position (left) and N wave for an exploding reflector at R position (right), ((Jäger et al., 2001).

A stereotomographic dataset consists of a dataset  $d$  with locally coherent events. It is a function of  $(x_S, x_R, p_S, p_R, t_{SR})_i$ , where  $x_S$  and  $x_R$  are the source and receiver locations,  $t_{SR}$  is the two-way traveltime,  $p_S$  and  $p_R$  are the local slopes at source and

receiver respectively (Lavaud et al, 2004). The slopes correspond to the horizontal component of the slowness vectors emerging at source and receiver. The other part of the stereotomography is the model  $m$ , described by pairs of ray segments and

a smooth velocity field  $V$ . Each pair of ray segments is a function of the parameters  $(X, \beta_S, \beta_R, t_S, t_R)$  so described by a reflection / diffracting point  $X$ , two emergence angles  $\beta_S, \beta_R$  towards the source and the receiver and two one-way traveltimes  $t_S, t_R$

from the point  $X$  toward the source and receiver (Lavaud et al., 2004).

The computing of the CRS stack does not depend on a macro-velocity model (Jäger et al., 2001), as opposed to the CMP stack. The CRS-stacking operator is defined as:

$$(1) \ t_{CRS}^2(x_0, h) = \left( t_0 + \frac{2 \cdot \sin \beta}{v_0} \cdot (x_{cmp} - x_0) \right)^2 + \frac{2 \cdot t_0 \cdot \cos^2 \beta}{v_0} \cdot \left( \frac{(x_{cmp} - x_0)^2}{R_N} + \frac{h^2}{R_{NIP}} \right)$$

where  $x_0$  is the output position,  $x_{CMP}$  is the position of midpoint between source and receiver  $(= (x_R + x_S)/2)$ ,  $h$  is the half offset  $(= (x_R - x_S)/2)$ ,  $v_0$  is the near surface velocity,  $t_0$  is the zero-offset two-way traveltime.

The three parameters  $(\beta, R_N$  and  $R_{NIP})$  define the stacking surface associated to the zero-offset traveltime,  $t_0$ . If the point  $P_0 = (x_0, t_0)$  is known, all we need is the near-surface velocity,  $v_0$  (Jäger et al, 2001). This parameter is assumed to be known, e.g. from other seismic studies performed in the studied area.

It has been shown that a CRS stack improves the signal-to-noise ratio and provides a better continuity of reflectors; this statement is based on synthetic and field data analyses. Each trace from the CRS stack is obtained by summing the traces from a super CMP gather so that a better noise attenuation is achieved. In addition, it is known that the procedure used to compute the CRS stack is also used to extract the information from the pre-stack data about the wavefront parameters; these parameters are determined for each point,  $P_0$ , of the zero-offset section (Jäger et al., 2001).

Once we have the CRS stack, an automatic traveltime picking is performed, as a first step of the post-stack stereotomography method; here,

only the locally coherent events are picked. The 2D velocity model is obtained after an iterative inversion process of the picked traveltimes; it is a smooth model and contains interval velocities as a function of depth. Then, the velocity model will be used for the pre-stack depth migration of the stacked seismic data.

### Seismic dataset: Acquisition and pre-processing

The post-stack stereotomography method is applied to a shallow land seismic dataset in order to get a more accurate velocity model necessary for the depth migration. The depth migrated section should show us a good depth image of the studied area, namely the proper positioning of the reflectors in depth. Before using this method, the land seismic data need a pre-processing in order to obtain common-midpoint (CMP) gathers having a signal-to-noise ratio as high as possible. The shallow seismic reflection dataset was recorded as a part of larger seismic survey. Dynamite was used as a source and the seismic information was recorded using vertical-component geophones (see Table 1 for the data acquisition parameters).



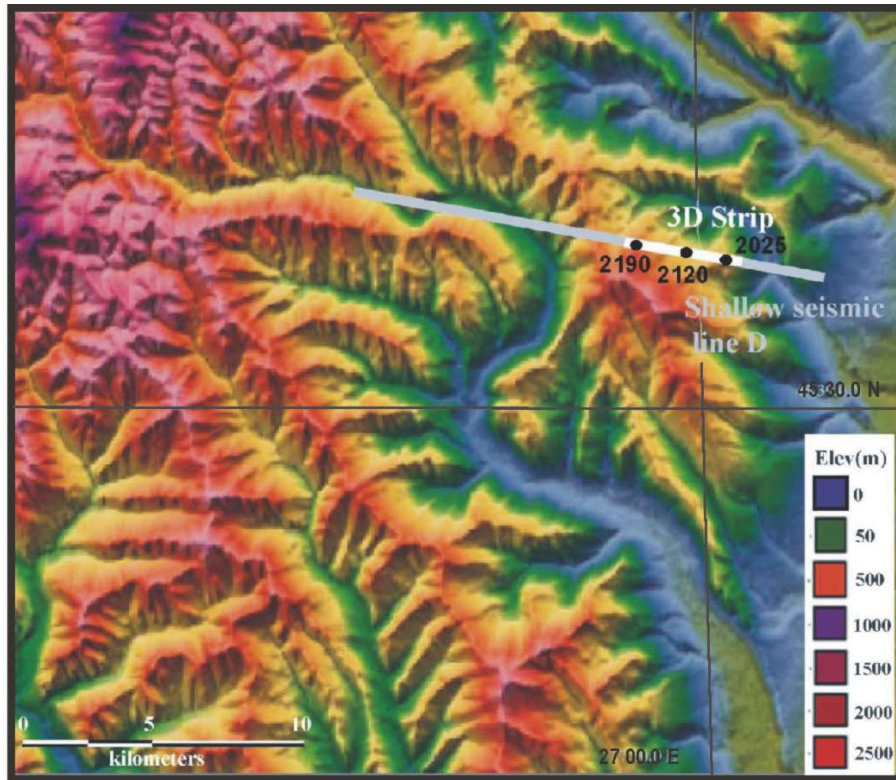


**Fig. 2.** Topographic map of the studied area (Dumitresti - Rm. Sarat)

In general, the quality of the seismic records is better toward the profile edges; clear reflectors can be seen even on the raw seismograms (see Fig. 4).

Table 1. Data acquisition parameters

Parameters	
Receiver spacing	5 m
Receiver number	160
Source spacing	20 m
Source type	dynamite
Source size	200 g
Source depth	2 m
Sampling time interval	1 ms
Time length	4 s

The static effects are important, they can be identified on the raw seismograms. The elevation values vary along the seismic profile; the spread of the receivers for the first shot (1 – 160) covered 800 m and the

maximum difference in elevation is 110 m (see Fig. 3). It is known, from previous seismic studies, that there are important near-surface velocity variations. Together with the elevation effect, they create statics that have to be extracted from the recorded data. A final datum of + 450 m has been chosen in order to compute the static corrections and a replacement velocity equal with 1750 m/s has been used.

The signal-to-noise ratio of the seismic data is enhanced by different filtering techniques (band-pass, FK, FX Deconvolution). First, we tried to remove the ground-roll from the analyzed dataset by applying the FK filter, followed by the other filters to eliminate the remaining noise (see Table 2 for the pre-processing steps).

## Improvement of seismic imaging in a low signal-to-noise area

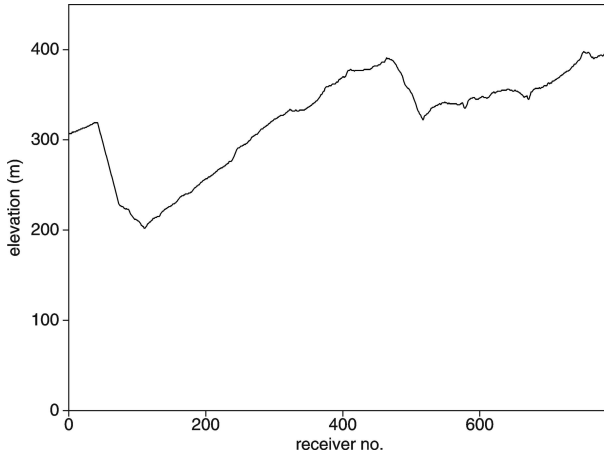
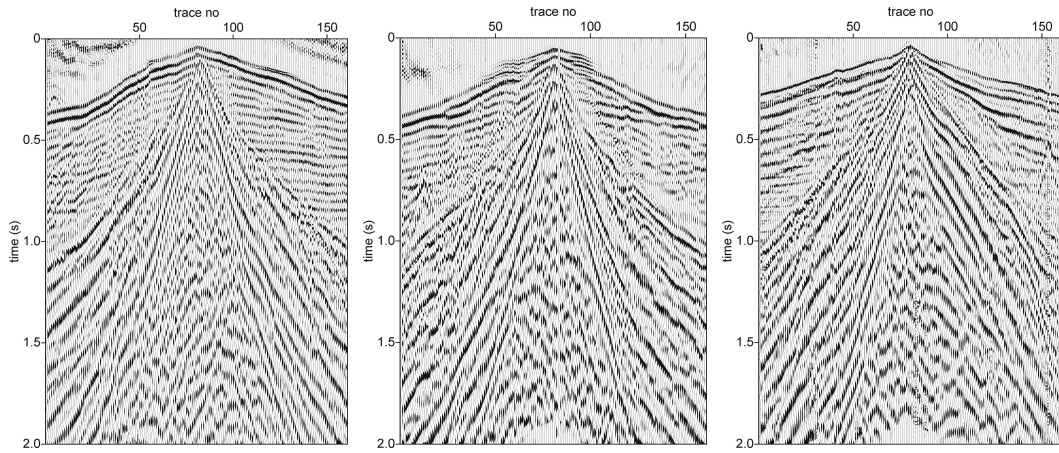


**Fig. 3.** Elevation variation along the seismic reflection profile

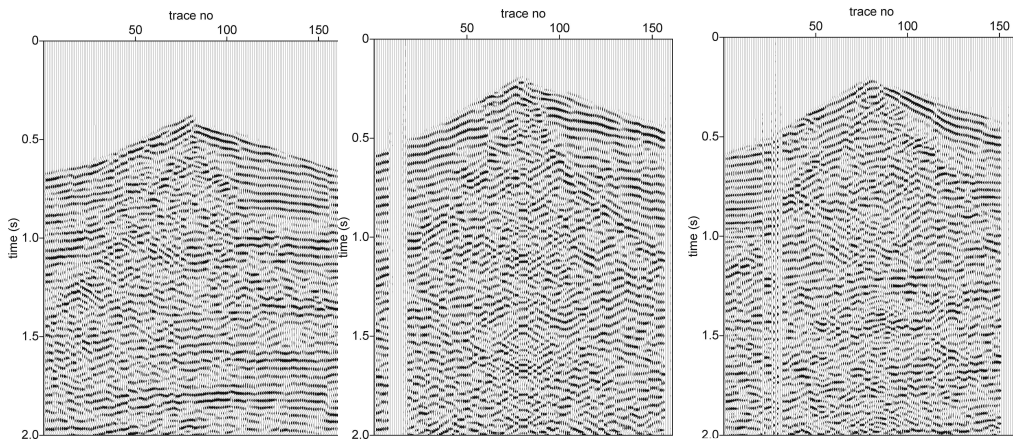
The top mute is used to remove refracted waves and noise before the first arrivals. Some of the very noisy traces were zeroed. The automatic gain control is used to normalize the energy along the traces. The full pre-processing flow is given in Table 2. In Figure 4 we display three of the most representative shots from the entire dataset and the results after pre-processing in Figure 5. The signal-to-noise ratio of these seismograms is indeed enhanced.

Table 2. Data pre-processing flow

Pre-processing steps	Parameters
Input seismic data	2 s trace length 157 shots
Geometry	2D land geometry
Static corrections	Replacement velocity = 1750 m/s Final datum = + 450 m
Desampling in time	2 ms
Trace muting	Top (first arrivals and noise before them)
Trace Kill/Reverse	Kill (very noisy traces)
Automatic Gain Control	300 ms
FK filter	Accept, fan polygon
Trace muting	Top (remaining noise)
Automatic Gain Control	300 ms
Band-pass frequency filtering	Zero phase, frequency, 20 – 24 – 64 – 72 Hz; Notch filter, 50 Hz, window 4 Hz
FX Deconvolution	Wiener Levinson, 500 ms, 20 – 70 Hz
2D Spatial Filtering	Convolutional method
Trace Muting	Top (remaining noise)
Trace Muting	Bottom (remaining noise)
Automatic Gain Control	300 ms



**Fig. 4.** Raw seismograms: 2025 (left), 2120 (center) and 2193 (right), (their positions on the seismic profile are shown in Fig. 2)



**Fig. 5.** Pre-processed seismograms with static corrections applied: 2025 (left), 2120 (center) and 2193 (right), (their positions on the seismic profile are shown in Fig. 2)

### Imaging using standard CMP-based approach

The standard velocity analysis was performed on the CMPs obtained from the pre-processed data (see Fig. 6). The un-migrated section, the CMP stack, is displayed in Figure 7 and its pre-stack depth migrated version in Figure 8; the Kirchhoff method is used for migration.

The seismic section from Figure 7 shows us a simple geological structure, with important geological interfaces characterized by a high contrast of acoustic impedance and represented by clear and high amplitude reflectors. The poor quality

of the stacked data on the center part of the section can be a result of many factors namely, the low signal-to-noise ratio of the input data, the presence of the surface waves and the elevation and near-surface effects. The elimination, by filtering, of the surface waves identified on a group of seismograms was difficult, even using the FK filter. Also, the elevation and near-surface effects are very important on this segment of the profile due to the field conditions (forrest, frequent elevation variations on small horizontal direction with large amplitude, lateral variations of the near-surface velocities).

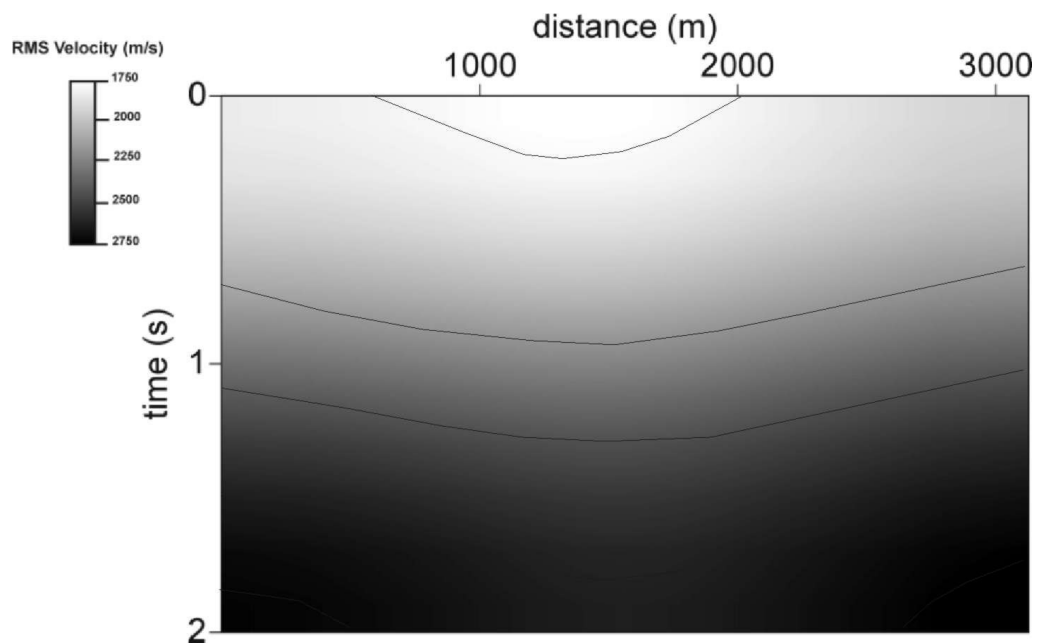


**Fig. 6.** 2D velocity model based on CMP velocity analysis

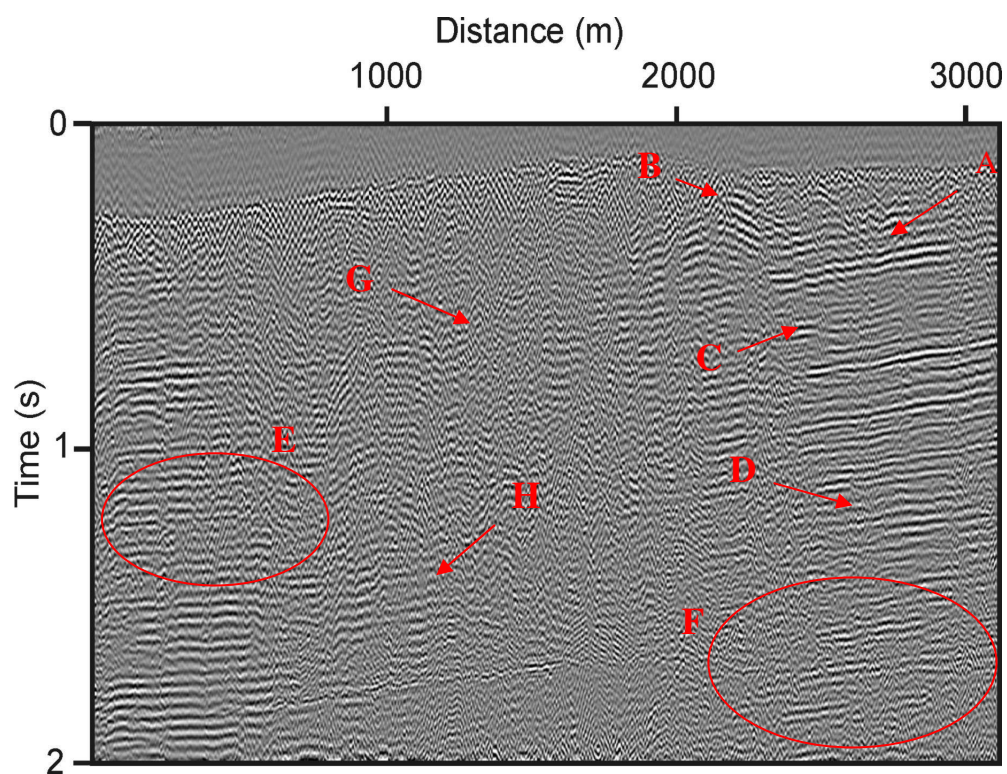


**Fig. 7.** Un-migrated time section using the CMP-based stacking approach

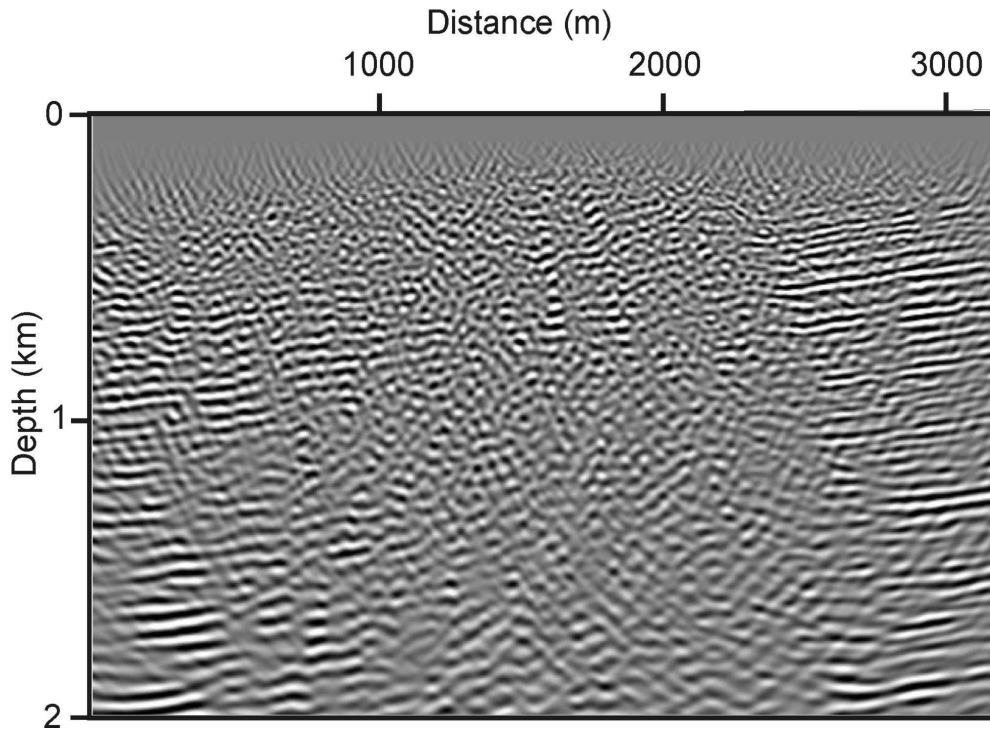


**Fig. 8.** Pre-stack depth migrated section using the standard CMP-based imaging approach, using interval velocities obtained from stacking velocities

We expect to obtain a higher quality of this segment of the seismic profile after the post-stack stereotomography, based on the

procedure used to compute the CRS stack and the 2D velocity model.

### Imaging using post-stack stereotomography

The CRS stack is a simulation of the zero-offset stack. The only difference between a CMP and CRS stack is the aperture used for stacking; the size of this aperture defines the number of the CMP gathers combined during stacking (multiple of CMP gathers in case of the CRS stack). The reflectivity of some areas characterized by low signal-to-noise ratio can be higher after this stacking (compare Fig. 7 and Fig. 9).

The CRS stack enhanced some reflectors; their amplitude and

continuity is more important compared to those from the CMP stack (see the group of reflectors C, D and F). As a counter-effect, the obtaining procedure of the CRS stack damaged the reflectivity of some areas, such as A, D and E. In addition, false reflectors (B) visible on the CMP stack, and unsupported by the known tectonic models for this area, were attenuated on the CRS stack. When we compare the center part of the CMP and CRS stacks we notice a higher reflectivity of the time interval 1.5 – 2 s, with clear short reflections (H); a reflector hard to follow on the CMP stack became more visible on the CRS stack (G).



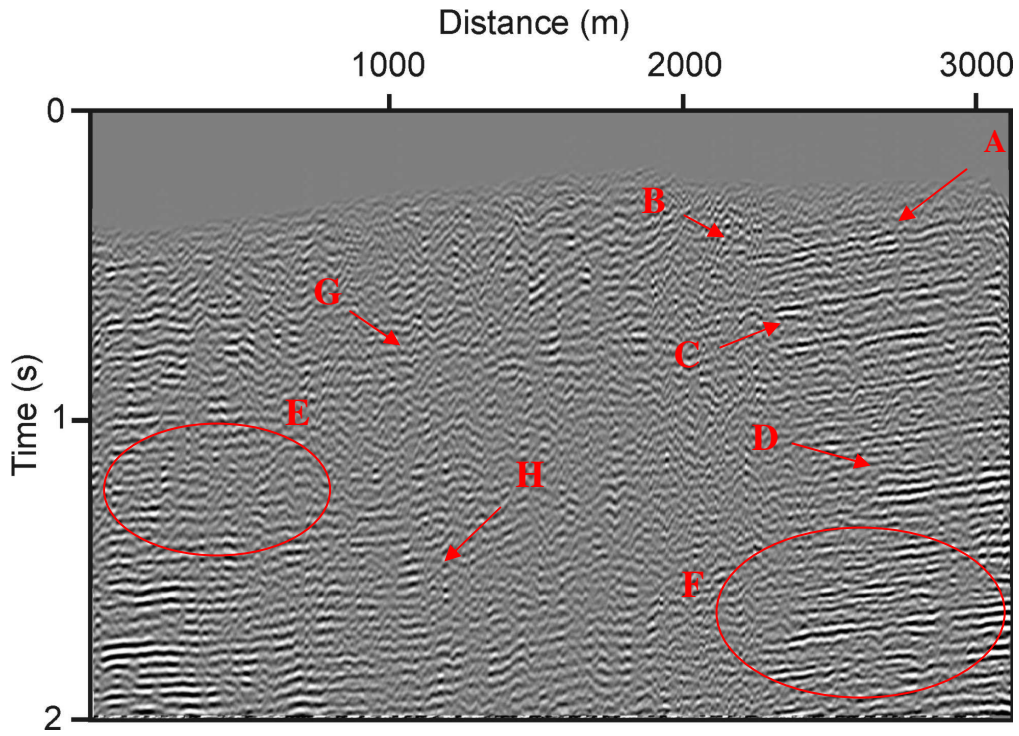


**Fig. 9.** Common-Reflection-Surface (CRS) stack

Another important section obtained during the computing of the CRS stack is the CMP coherency section (see Fig. 10). This section shows us high coherency values (red areas) where the reflections are stronger than in the rest of the section;

in these areas, the corresponding attributes are considered reliable (Jäger et al., 2001). By comparing the CMP stack and the CMP coherency section we can separate the real events from those considered noise.

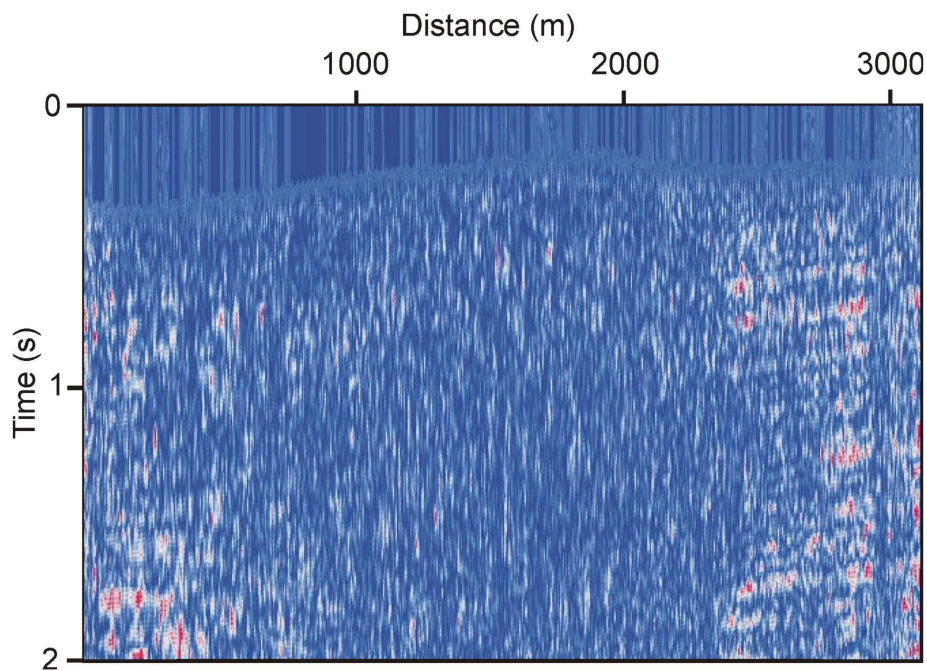


**Fig. 10.** The CMP coherency section

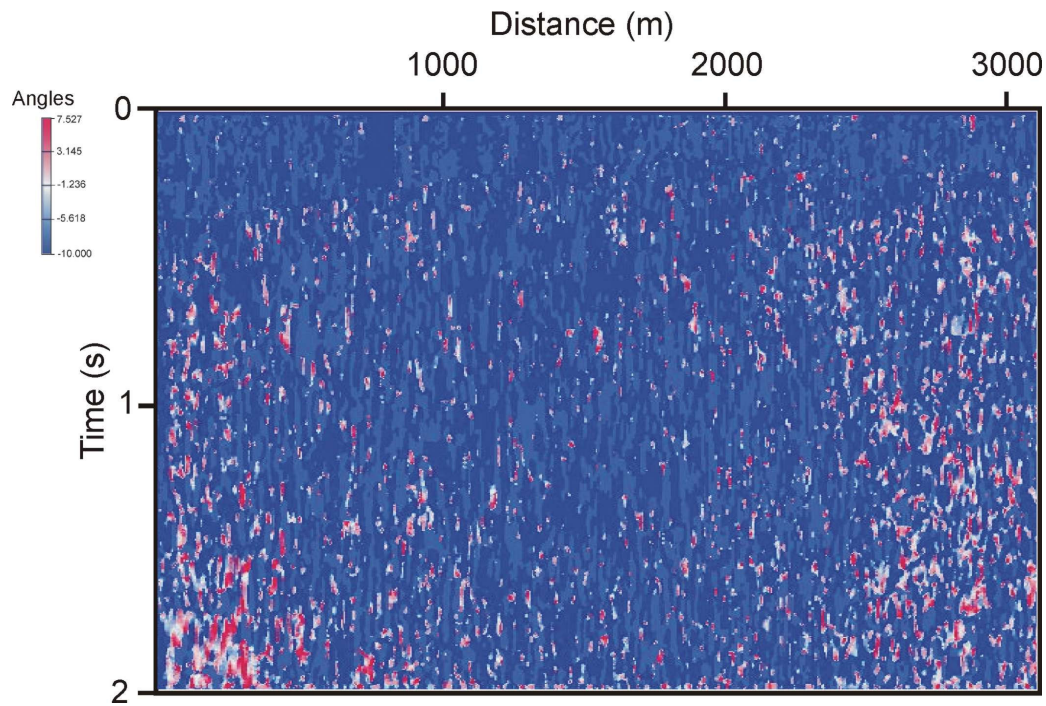


**Fig. 11.** Angle section

An important parameter used in inversion is the angle  $\beta$  that is determined for each point of the CRS section. The higher angle values correspond to those areas where the

reflectors are clear, with high amplitude and more continuous (red areas in Fig. 11); these zones contain reliable angle information (Jäger et al., 2001).

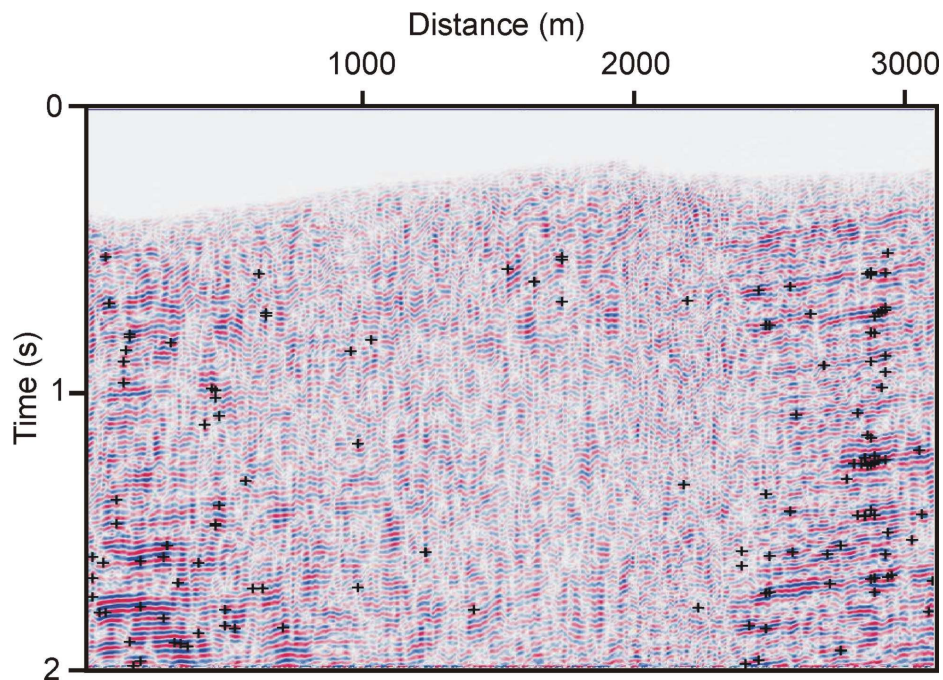


**Fig. 12.** Automatically picked traveltimes

Having all this information, the locally coherent events are

automatically picked (see Fig. 12). A half-window of 400 m and a

semblance threshold of 0.75 are used for picking. Just a few events were picked on the center part of the section because of the lack of the continuous reflectors. The 2D velocity model is determined after the picked traveltimes

inversion (see Fig. 13); the cell size is 200 m and a number of 10 iterations have been done. It is a smooth velocity model and it contains interval velocities as a function of depth.

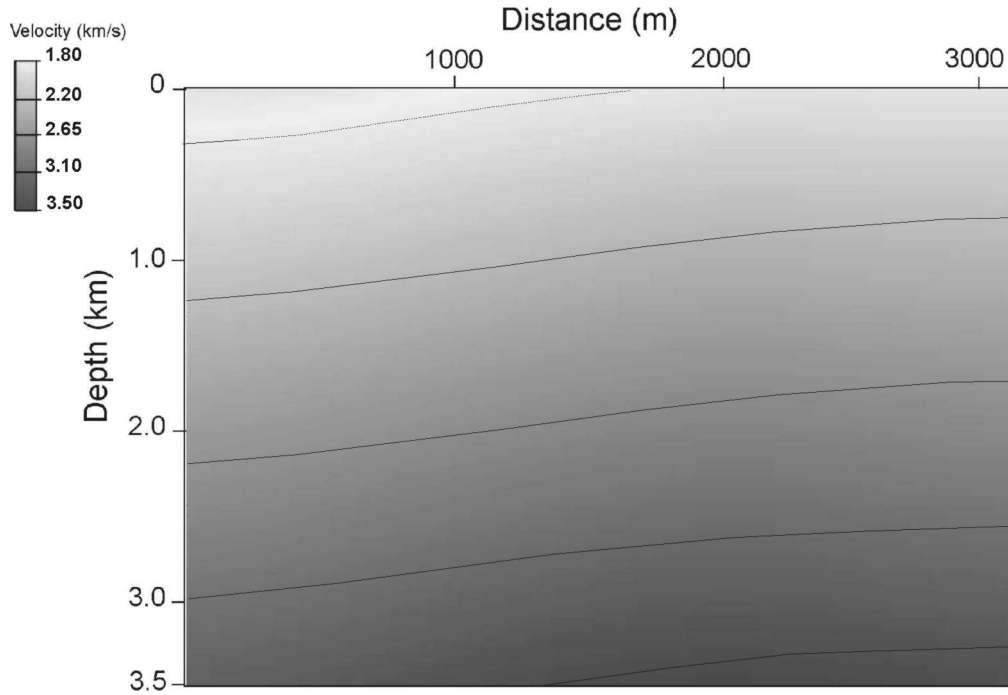


**Fig. 13.** 2D velocity model from post-stack stereotomography

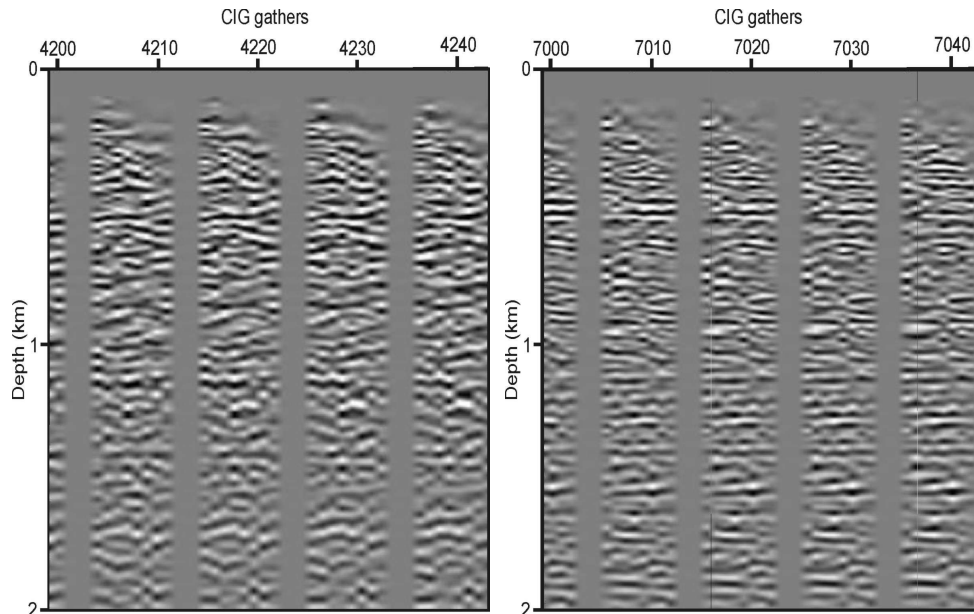


**Fig. 14.** Common-Image-Gathers from the central part (left) and right end (right) of the profile

The velocity model obtained from stereotomography is then used for

a pre-stack depth migration, again using the Kirchhoff migration method.



During this migration we have the possibility to verify the accuracy of the velocity in different points of the model. Two groups of Common-Image-Gathers (CIG) gathers were selected from two locations along the profile (see Fig. 14); the traces in each CIG gather are sorted after offset. After an analysis of some CIG gathers, we can say that good velocity values are obtained on the gathers that

contains flat events (see Fig. 14, right); these gathers correspond to the data recorded on the eastern part of the profile which contains clear reflectors. The CIG gathers chosen from the central part of the profile do not show us clear flat reflectors, so we can not decide if the velocity values, at these locations, are good or not (see Fig. 14, left).

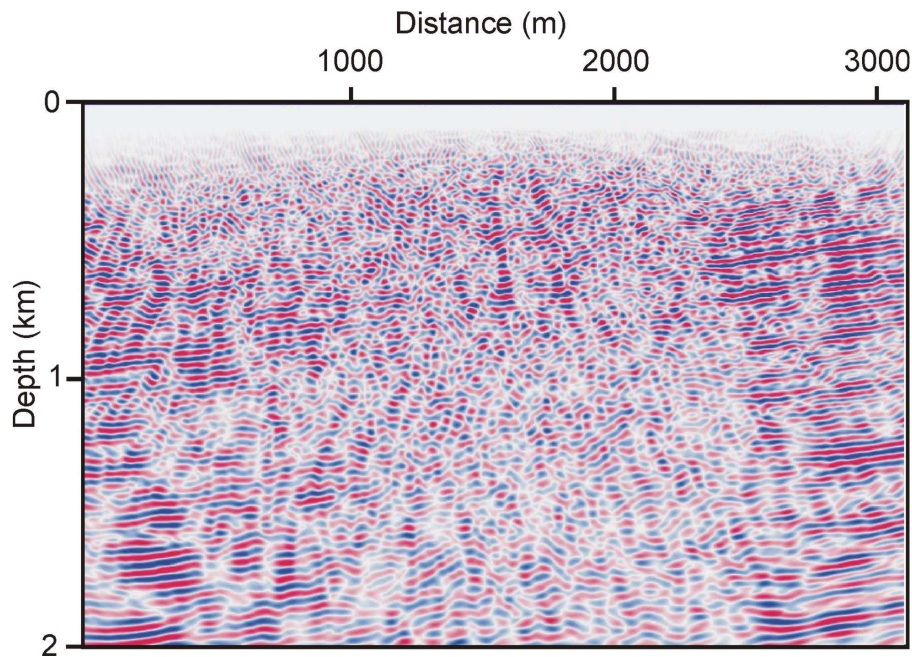


**Fig. 15.** Pre-stack depth migrated stack with velocity model from traveltimes inversion of picked events on CRS stack

The result of the depth migration is displayed in Figure 15. It shows, still, a poor continuity of the reflections in the central part of the seismic section, but higher than that from the standard procedure output. By looking at the reflection patterns we notice a difference between the frequency content of the signal on the left part and the right part of the seismic section (see Fig. 8 and, also, Fig. 15). This can be explained by lateral facies variation of the Quaternary and Upper-Pliocene deposits; in addition, the tectonic models known for this area do not

show the presence of important faults or faulting area that could be responsible for the poor quality of the data on the central part of the profile.

### Conclusions

The post-stack stereotomography method was used to determine an accurate 2D velocity model necessary for stacking and depth migration. The standard processing flow did not provide a very good velocity model and a CMP section that shows us clear information about the

geological structure of the studied area (only toward the edges of the profile). The low signal-to-noise ratio of the input data, maybe a consequence of the field conditions, can be responsible for the lack of the clear reflections on the central part of the profile. The reflectivity of this segment is somehow enhanced on the CRS stack. In addition, groups of reflections show a greater amplitude and continuity on the CRS stack compared with those seen on the CMP stack; other areas from the CRS stack show an interrupted continuity of the reflectors, while this continuity is clear on the standard processing result.

The output of the post-stack stereotomography shows an improved seismic section image, due to the improved velocity model quality. The accuracy of the 2D velocity model used for the pre-stack depth migration could be verified after a CIG gathers analysis; based on this, we can conclude that the velocity values determined especially toward the edges of the profile are good, which means that the depth migration worked well and we have a correct positioning in depth of the reflectors / geological interfaces.

### Acknowledgements

The authors thank to the OPERA team for their help and fruitful comments. Special thanks are due to Dr. Bertotti and Dr. Matenco for their support during the seismic data acquisition. This research was sponsored by the Netherlands Research Centre for Integrated Solid Earth Sciences (ISES).

### References

- Billette, F. and Lambaré, G., 1998, Velocity macro-model estimation from seismic reflection data by Stereotomography. *Geophy. J. Int.*, 135(2), pp 671 – 680.
- Billette, F., Le Bégat, S., Podvin, P. and Lambaré, G., 2003, Practical aspects and applications of 2D Stereotomography. *Geophysics*, 68 (3), pp 1008 – 1021.
- Chalard, E., Podvin, P., Le Bégat, S., Berthet, P. and David, B., 2002, 3D stereotomographic inversion on a real dataset, 72<sup>nd</sup> annual SEG meeting, Expanded Abstracts, pp 946 – 948.
- Chauris, H., Noble, M., Lambaré, G. and Podvin, P., 2002a, Migration velocity analysis from locally coherent events in 2-D laterally heterogeneous media, Part I: Theoretical aspects, *Geophysics*, 67(4), pp 1202 – 1212.
- Duvenek, E. and Hubral, P., 2002, Tomographic velocity model inversion using kinematic wavefield attributes, 72<sup>nd</sup> annual SEG meeting, Expanded Abstracts, pp 862 – 865.
- Jäger, R., Mann, J., Höcht, G. and Hubral, P., 2001, Common-reflection-surface stack: Image and attributes, *Geophysics*, Vol. 66, No. 1, pp 97 – 109.
- Lambaré, G., Alerini, M. and Podvin, P., 2004, Stereotomographic picking in practice, Expanded Abstracts, EAGE conference.
- Lavaud, B., Baina, R. and Landa, E., 2004, Poststack stereotomography: a robust strategy for velocity model estimation, Expanded Abstracts, EAGE conference.